Molecular Structures in Isotactic Polystyrene Thermoreversible Gels

Marc Klein,† Annie Brûlet,‡ and Jean-Michel Guenet*

Laboratoire de Spectromètrie et d'Imagerie Ultrasonores, Université Louis Pasteur, CNRS UA 851, 4, rue Blaise Pascal, F-67070 Strasbourg Cedex, France. *Received March 1, 1989; Revised Manuscript Received June 7, 1989*

ABSTRACT: The chain helical structure, the chain–solvent arrangement, and the chain trajectory are investigated in isotactic polystyrene (iPS) thermoreversible gels by three techniques: neutron diffraction, swelling experiments, and small-angle neutron scattering. From the neutron diffraction experiments on gels prepared from various solvents, it is again concluded that the 12_1 helical form is absent in the nascent state (undried and unstretched). As already proposed in a previous paper, a solvated near-3_1 helix seems to be a better candidate to account for the results (ladderlike model). The swelling experiments support this model by indicating that the gel behaves as a polymer–solvent compound whose stoichiometry is defined at $C_\gamma \approx 0.3$ in *cis*-decalin and $C_\gamma \approx 0.38$ in *trans*-decalin, values in good agreement with those found previously by calorimetry and solvent crystallization. The small-angle neutron scattering on iPS/*cis*-decalin gels reveals a most unusual behavior in that the chains become stiffer and stiffer up to $C = 0.3$ (increase of the chain radius of gyration and q^{-1} behavior consistent with rodlike portions larger than 300 Å) then lose their stiffness (decrease of the chain radius of gyration and loss of the q^{-1} behavior). Such behavior is in accord with the temperature–concentration phase diagram established earlier. All the results are discussed in the light of various molecular models.

Introduction

Investigations on the molecular structures involved in iPS thermoreversible gels have provided one with numerous results that have raised several questions. Different answers have been put forward, leading eventually to conflicting models.[1-5]

Girolamo et al.,[1] after discovering by X-ray diffraction a new reflection at 0.51 nm on partially dried and stretched gels, first inferred that gelation might arise from stereoregularity defects on the chain. Later they accounted for the 0.51 reflection through the existence of a new helical form: 12_1 with a 6-fold symmetry.[2]

To explain why a new helical form could be formed in gels rather than the usual 3_1 helical structure, Sundararajan et al.[3] proposed this form to be stabilized by solvent molecules, that is solvated helices and correspondingly solvated crystals.

More recently, Guenet[4] showed by means of neutron diffraction experiments, for which only the polymer was labeled, that the 0.51-nm reflection was in fact not characteristic of the polymer but could be found in liquid decalin. From simple geometrical argument, Guenet, while retaining the idea of helix solvation, considered a near-3_1 form.[4] The nascent gel diffraction pattern, which is reminiscent of liquids, led to a structure (ladderlike model) closer to nematic liquid-crystalline than crystalline polymers. From neutron scattering experiments intended to determine the chain conformation, it was found that the chains adopt a wormlike structure with a statistical element of about 8 nm.[6] This structure is similar to what is known for liquid-crystalline polymers and gives further credit to the ladderlike model. More recently, however, the helix solvation has been questioned on the basis of NMR experiments.[5]

In this paper, we further test these models through three types of experiments: (i) neutron diffraction experiments on other solvents known to produce physical gels to discover whether the 0.51-nm reflection is also absent; (ii) swelling experiments; (iii) neutron scattering investigation on the chain conformation as a function of polymer concentration in relation with the temperature–concentration phase diagrams established previously.[7]

Experimental Section

(A) Material. The isotactic polystyrene (iPS) samples were all synthesized following the Natta method[8] and are over 99% isotactic.[9]

Two hydrogenated samples were used: iPSK, $M_w = 3.2 \times 10^5$, $M_w/M_n \approx 2.8$; iPSG, $M_w = 1.38 \times 10^5$, $M_w/M_n \approx 1.2$.

The characteristics of the deuterated samples are given in Table I.

High-purity grade protonated *cis*-decalin was purchased from Merck Laboratories, while the deuterated *cis*-decalin was obtained from the Janssen company and is deuterated over 99%. All the solvents were employed without further purification.

(B) Sample Preparation. A mixture of polymer and solvent was heated up to 175 °C in a test tube. Once a clear solution was obtained the gels were prepared by either quenching at 0 °C and keeping the sample at this temperature for 30 min or quenching at 14 °C and keeping the sample at this temperature for 2 h. For the neutron scattering experiments the solutions were cast in a mold described elsewhere,[6] allowing the preparation of disk-shaped samples of 1-mm thickness and 1.5-cm diameter. For the neutron diffraction experiments the gels were prepared in NMR silica tubes of 4-mm diameter sealed from the atmosphere. For the swelling experiments, cylinder-shaped samples of 1-cm height and 1-cm diameter were cut off from a gel slab obtained in the same type of mold as that employed for preparing the neutron scattering samples.

(C) Neutron Scattering. 1. Setup. The experiments were performed at the high-flux reactor of the Institute Laue-Langevin (ILL, Grenoble, France) on D11 and D17 small-angle cameras. The transfer momentum $q = 4\pi/\lambda[\sin \theta/2]$ (λ = neutron wavelength and θ the scattering angle) was in the range $5 \times 10^{-3} \leq q$ (Å^{-1}) $\leq 1.5 \times 10^{-2}$ for D11 ($\lambda = 10$ Å) and $10^{-2} \leq q$ (Å^{-1}) $\leq 1.3 \times 10^{-1}$ for D17 ($\lambda = 12$ Å).

A mechanical wavelength selector was used on both apparatus, providing a wavelength distribution characterized by $\Delta\lambda/\lambda \simeq 9\%$.

The gels were held in quartz containers (22-mm outer diameter, 19-mm inner diameter, and 1-mm thickness). The experiments were carried out at 18 ± 1 °C.

The experiments on the all-labeled samples were carried out at the Laboratoire Léon Brillouin (CEA-CNRS) at Saclay on

† Institut Charles Sadron, F-67083 Strasbourg Cedex, France.
‡ Laboratoire Léon Brillouin CEN Saclay, F-91191 GIF/YVETTE Cedex, France.

0024-9297/90/2223-0540$02.50/0

Table I
Molecular Weights of the Deuterated Samples from GPC in THF at 20 °C and from Small-Angle Neutron Scattering (SANS) on Gels Prepared at 0 °C[a]

sample	M_{wGPC}	M_w/M_{nGPC}	M_{wSANS} (22.5%)	M_{wSANS} (30%)	M_{wSANS} (40%)
D0.74	7.4×10^4	1.1	6×10^4	5.6×10^4, 5.4×10^4 [a]	6×10^4
D1.5	1.5×10^5	1.13	1.2×10^5	9×10^4, 1.1×10^5 [a]	1.1×10^5
D2.5	2.5×10^5	1.15	2.2×10^5	2.2×10^5, 2.2×10^5 [b]	2×10^5
D0.6	6.0×10^4	1.1			

[a] The overall polymer concentration is given in parentheses. [b] Gels prepared at 14 °C.

PAXY. A mechanical wavelength selector was also used, providing a wavelength distribution characterized by $\Delta\lambda/\lambda \simeq 8\%$. With $\lambda = 5$ Å the transfer momentum was in the range $1.5 \times 10^{-2} \leq q$ (Å^{-1}) $\leq 1.3 \times 10^{-1}$.

2. Signal Processing. In order to measure the coherent scattering from the deuterated chains only, a mixture of D + H decalin was used (21.3% D decalin + 78.7% H decalin), the scattering of which matches that of protonated polystyrene.[6] The scattered intensities were corrected for sample transmission. As usual, a blank signal, scattered by a mixture of hydrogenated polymer and a blend of deuterated and hydrogenated solvent (same composition as above) was removed from the total scattered intensity to correct for incoherent scattering. Finally, the spectra were normalized by an incoherent spectrum scattered by protonated water. The normalized intensity then reads

$$I_N(q) = KC_D M_w S_D(q) \quad (1)$$

where C_D is the concentration of labeled material, M_w the weight-average molecular weight, and $S_D(q)$ the scattering function of the deuterated chains. K is a constant, which presently is given as

$$K = [4\pi\delta N_A(a_H - a_D)^2]/[M_D^2(1 - T)] \quad (2)$$

where δ is the water-sample thickness (in cm), N_A is Avogadro's number, M_D is the monomer molecular weight, T is the water transmission, and a_H and a_D are the scattering lengths (in barns) of the deuterated species and of the mixture iPSH + D decalin + H decalin, respectively.

(D) Neutron Diffraction. The experiments were performed at the ORPHEE reactor located at the Laboratoire Leon Brillouin (LLB, CEN Saclay, France) on the spectrometer 7C2 equipped with a banana-type detector made up of 640 cells with an angular resolution of 0.2°. We used cold neutrons with a wavelength of 1.095 Å obtained from reflection of the primary beam onto the (111) plane of a Germanium crystal. The scattering vectors available ranged from 0.25 to 10 Å^{-1}. The signal was normalized by both a vanadium sample and a plexiglas sample. Further details on the apparatus are available on request.

(E) Swelling Measurements. Appropriate samples were immersed in an excess of solvent. The swelling degree G was taken as the ratio of the sample weight after a given time t over the sample weight prior to immersion. The equilibrium swelling degree G_∞ was determined when the sample no longer swelled. All the experiments were carried out at room temperature.

Results and Discussion

(A) Neutron Diffraction. In a previous paper,[4] it had been observed from neutron diffraction experiments carried out on iPS/*cis*-decalin gels that the 0.51-nm reflection observed by X-ray diffraction on these gels and assigned to a new helical form (12_1 helix) was not found in the nascent gel. The fact reported by Keller et al.[10] that a thorough removal of the preparation solvent usually leads to the disappearance of this reflection is in agreement with these conclusions. Yet, for one solvent, i.e., *trans*-decalin, supposedly decalin-free samples are reported to still exhibit this reflection when examined by X-ray diffraction.[10]

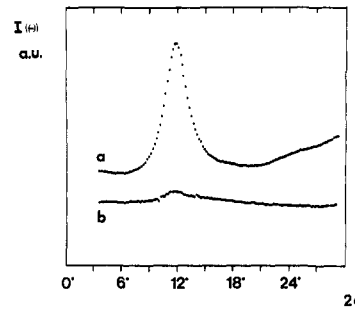

Figure 1. Neutron diffraction patterns for deuterated (a) and hydrogenated *cis*-decalin (b). Intensity in arbitrary units.

As a result, the question still holds as to whether the 0.51-nm reflection could also be present in the nascent gel state, undried and unstretched.

To answer these questions and to supplement previous findings, we have carried out a series of neutron diffraction experiments on iPS/*trans*-decalin gels as well as on other systems.

1. Principle of the Experiments. The use of either hydrogenated or deuterated samples allows one to modify the diffraction power of the constituents of a system in a neutron diffraction experiment.[11] Figure 1 shows the attenuation of the first diffraction maximum when hydrogenated decalin is used in lieu of deuterated decalin.

This property is particularly interesting when polymers composed of hydrogen and carbon are dealt with. If all the species have the same type of labeling, either deuterated or hydrogenated, a neutron diffraction experiment yields results quite similar to those obtained by X-ray diffraction. Conversely, if one component is deuterated, the other one being still protonated, then the diffraction power of the former will be enhanced by at least a factor of 4 ($b_D^2/b_H^2 \approx 4$). Making use of this property, the polymer structure can be investigated by using a deuterated polymer and a hydrogenated solvent. As a result, the drying process is no longer necessary.

The intensity is given as

$$I(q) = \bar{A}_p^2(q)S_p^{coh}(q) + \bar{A}_s^2(q)S_s^{coh}(q) + 2\bar{A}_s(q)\bar{A}_s(q)S_{ps}^{coh}(q) + S_p^{inc} + S_s^{inc} \quad (3)$$

where A_s and A_p are the structure factor of the solvent and the monomer, respectively, S^{coh} the coherent scattering functions, and S^{inc} the incoherent scattering. The deuterated polymer incoherent signal is usually very small and thereby neglected.

While the solvent intensity is strongly attenuated, it is not negligible and must be accordingly removed. A measure on the only solvent gives

$$I_s(q) = \bar{A}_s^2(q)S_s^{coh}(q) + S_s^{inc} \quad (4)$$

Once this intensity is properly substracted from (3), $I(q)$ is

$$I(q) = \bar{A}_p^2 S_p^{coh}(q) + 2\bar{A}_s(q)\bar{A}_p(q)S_{sp}^{coh}(q) \quad (5)$$

This is almost the intensity diffracted by the polymer, except for the cross-term. This term is usually weaker and should not have any bearing in the present case.

As detailed above, 7C2 is a high-resolution spectrometer. In order to detect with certainty the weakest reflections, the number of counts/cell was never lower than $N = 10^5$. This means that the statistical dispersion $N^{1/2}/N$ was lower than 0.3%.

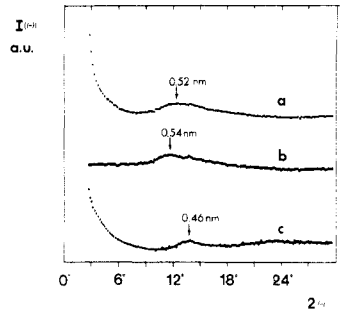

Figure 2. Neutron diffraction patterns of (a) iPSD/*trans*-decalinH gel (D2.5, C_{pol} = 37%), (b) liquid protonated *trans*-decalin, and (c) the difference of (b) from (a). Intensity in arbitrary units.

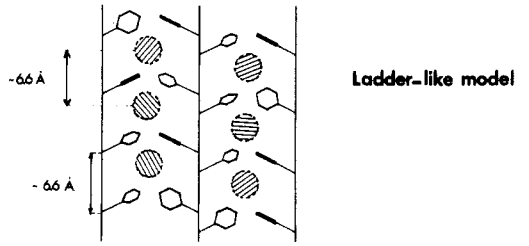

Figure 3. Schematic representation of the ladderlike model. The phenyl rings are purposely oriented at random on the C–C axis to emphasize that the chain conformation is not strictly a 3_1 helix. The hatched circles stand for the solvent molecules. Here too, the hatching is at random to illustrate the absence of orientation of the solvent molecules.

2. Results. Results obtained on iPSD/*trans*-decalin gels are reported in Figure 2. A maximum is seen at 0.52 nm (Figure 2a). Yet, *trans*-decalin in the liquid state exhibits a maximum at 0.54 nm (Figure 2b). Once the *trans*-decalin signal is substracted from that of the iPSD/*trans*-decalin gel, the intensity displays a broad maximum at 0.46 nm (Figure 2c). There is no detectable sharp peak at 0.51 nm that would reveal the presence of 12_1 helices. As in a previous publication[4] we accordingly conclude that this helix is not characteristic of the gel structure in the nascent state.

As was emphasized elsewhere, the first maximum for a liquid is related to the distance between first neighbors.[12] This distance d can be estimated from

$$1.23\lambda = 2d \sin \theta/2 \quad (6)$$

As with *cis*-decalin, for *trans*-decalin we end up with $d \approx 0.66$ nm. This value is very close to the pitch of the 3_1 helix (0.665 nm[13]). We thus conclude again that the polymer adopts a conformation close to the 3_1 helix, yet not regularly arranged as in crystals (see Figure 3). If the chain are under a near-3_1 conformation, then the solvent first-neighbor molecules can be in close contact, allowing maximum space filling. This model, designated as a ladderlike model, is similar to a molecular model proposed by Watanebe et al.,[14] where the incorporation of solvent molecules into the α-helical form of poly(γ-methyl L-glutamate) is considered.

We have further examined other systems that are known to produce physical gels (Figure 4).

iPSD/1-Chlorodecane and iPSD/Hexahydroindan. The diffraction pattern of the iPSD/1-chlorodecane gel (Figure 4a) does not reveal any sharp peak or maximum at 0.51 nm, even before solvent signal substraction. For the iPSD/hexahydroindan gel (Figure 4c), one perceives that the solvent is also responsible for the maximum at 0.52 nm.

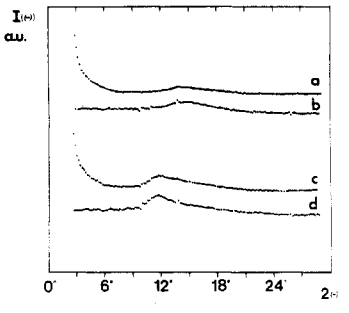

Figure 4. Neutron diffraction patterns for (a) iPSD/1-chlorodecaneH gel (D0.6, C_{pol} = 49%), (b) liquid 1-chlorodecaneH, and (c) iPSD/hexahydroindanH gel (D2.5, C_{pol} = 28%). Intensity in arbitrary units.

Thus we have now studied four systems by the neutron diffraction technique together with the deuterium labeling method. In all cases no sharp reflection near 0.51 nm has been observed.

Here we want to emphasize that we do not conclude that 12_1 does not exist. There are numerous evidences by Keller et al.[2] in favor of it. It would, however, be of interest to discover the growth mechanism of this helix if it is not present in the gel in the first place.

(B) Gel Swelling. The swelling experiments consist of immersing a piece of gel in an excess of preparation solvent. An equilibrium swelling ratio G_∞ is defined as

$$G_\infty = P_\infty/P_0 \quad (7)$$

where P_0 is the weight of the gel sample as-prepared and P_∞ its weight after reaching equilibrium.

Provided the piece of gel absorbs solvent without losing any polymer chains, an equilibrium concentration C_{equ} can be defined as a function of the preparation concentration C_{prep}:

$$C_{equ} = G_\infty^{-1} C_{prep} \quad (8)$$

Results (C_{equ} versus C_{prep}) are given in parts a (*cis*-decalin) and b (*trans*-decalin) of Figure 5. As can be seen, two regimes are present in both systems: for $C < C_\gamma$, there is no significant swelling and $C_{equ} \approx C_{prep}$; for $C > C_\gamma$, the gels always swell to the same equilibrium concentration independent of the preparation concentration C_{prep}.

Further, the value determined for this equilibrium concentration is $C_\gamma \approx 0.28$ in *cis*-decalin and $C_\gamma \approx 0.38$ in *trans*-decalin.

These results lead one to the following comments: (i) The swelling behavior is typical of and indeed very close to what one would theoretically expect for polymer–solvent compounds. As a matter of fact, as long as the stoichiometry is fulfilled, that is for $C_{prep} < C_\gamma$, there is no need for the system to absorb solvent unless there were a large amount of "amorphous" domains. Conversely, for $C_{prep} > C_\gamma$, the system tends to reach stoichiometric conditions, hence solvent absorption takes place.

Accordingly, the theoretical behavior for a perfect polymer–solvent compound will be $C_{equ} = C_{prep}$ for $C < C_\gamma$ and $C_{equ} = C_\gamma$ for $C > C_\gamma$.

For systems made up with solvent-free crystalline regions (no polymer–solvent compound formed) alternating with amorphous regions that are liable to absorb solvent, G_∞ reads[15]

$$G_\infty = 1 + (C_\alpha/C_\gamma - 1)C_{prep}/C_\alpha \quad (9)$$

where C_α is the polymer-rich phase initial concentration and C_γ its concentration after swelling to equilibrium.

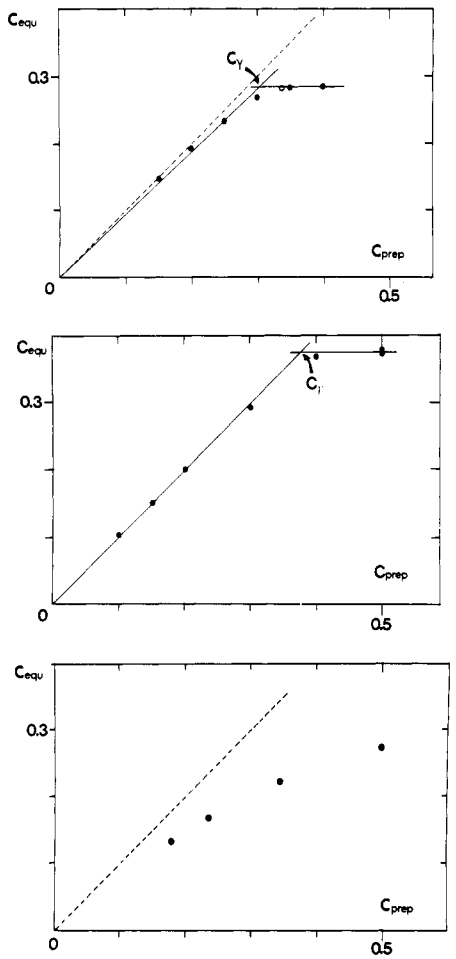

Figure 5. Equilibrium concentration C_{equ} versus preparation concentration C_{prep} for (a) iPS/*cis*-decalin gels [(●) iPSK, (○) iPSG], (b) iPSK/*trans*-decalin gels, and (c) a copolymer/*trans*-decalin gel (from ref 15). In all cases the dotted line stands for $C_{equ} = C_{prep}$.

The behavior described by relation 9 has already been observed with gels of multiblock copolymers (Figure 5c) for which it is known that the crystalline regions are solvent free.[15] Unlike the polymer–solvent compound, the swelling behavior exhibits here an increasing departure from the law $C_{equ} = C_{prep}$ with increasing concentration. Further, no asymptotic behavior is reached.

(ii) The value of C_γ determined by means of this method is close to those found from the gel formation and/or the gel melting enthalpies[7] ($C_\gamma \approx 0.28$–0.3 in *cis*-decalin and $C_\gamma \approx 0.4$ in *trans*-decalin) or from the solvent crystallization method[4] ($C_\gamma \approx 0.28$ in *cis*-decalin and $C_\gamma \approx 0.4$ in *trans*-decalin).

(C) Neutron Scattering. 1. A Few Chains Are Labeled. The excess, normalized scattered intensity is expressed in the Zimm approximation:[16]

$$I_N(q) = KC_D M_w[P(q) - 2A_2C_D P^2(q)] \quad (10)$$

where C_D, M_w, and K have the same meaning as in (1), $P(q)$ is the chain form factor, and A_2 is the virial second coefficient. In the Guinier domain ($qR < 1$), $I_N(q)$ reduces to

$$I_N(q) = KC_D M_w[1 - q^2\langle R_g\rangle^2/3][1 - 2A_2C_D] \quad (11)$$

Usually, the form $C_D I_N^{-1}(q)$ is preferred:

$$KC_D I_N^{-1}(q) = [1/M_w(1 + q^2\langle R_g\rangle^2/3)] + 2A_2C_D \quad (12)$$

In this representation, linearity can be experimentally obtained for $qR > 1$. For instance, R_g for a Gaussian chain is measured to within 10% up to $qR \simeq 3$. However, for highly branched polymers or compact structure the departure from linearity is already seen for $qR < 1$, which entails that the condition $qR \ll 1$ must be strictly fulfilled.

It must be stressed that polydispersity tends to broaden the domain over which linearity can be achieved.

In the asymptotic domain, the intensity usually reduces to

$$I_N(q) \propto q^{-n} \quad (13)$$

where n is an exponent that depends upon the chain trajectory.

For some models of chain trajectory analytical expressions are available that allow one to calculate the entire scattering pattern from the Guinier range to the asymptotic domain. Calculations are detailed in the Appendix for models that are relevant to the present article.

In this section only the system iPS/*cis*-decalin has been investigated. In the Guinier domain the chain radius of gyration, R_g, has been studied as a function of the overall polymer concentration. R_g has been determined by the Zimm method with three labeled chains concentrations: 0.01, 0.02, and 0.03 g/cm^3 (concentration per centimeter cubed of gel). Values of M_w obtained from SANS are given in Table I and values of R_g in Table II. As can be seen, the weight-average molecular weights measured from neutron scattering are in good agreement with those obtained from GPC.

The variation of R_g with the overall polymer concentration is shown in Figure 6. In spite of the large uncertainty on the absolute value of R_g arising from the fact that the condition $qR_g < 1$ is not strictly fulfilled, there is unmistakably a maximum located at $C_{pol} = 30\%$. This behavior is most unusual. In amorphous polymers, R_g decreases with concentration as $C^{-1/8}$.[17] In crystalline polymers, although there are no available data so far, one would not expect R_g to increase then to decrease with increasing polymer concentration. As a matter of fact, in dilute solutions the chain tends to be well organized, which entails a high value of R_g,[18,19] while in the bulk

Table II
Values of the Radius of Gyration R_g (Å) as a Function of Gel Concentration[a]

sample	15%[b]	22.5%	30%	40%
D0.74	200 ± 10	252 ± 20	308 ± 25	220 ± 20
D1.5	267 ± 25	274 ± 20	300 ± 25	264 ± 30
D2.5	332 ± 30	368 ± 40	448 ± 60	401 ± 50

[a] Values for 30% gels prepared at either 0 or 14 °C are indistinguishable within experimental uncertainties. [b] From ref 6.

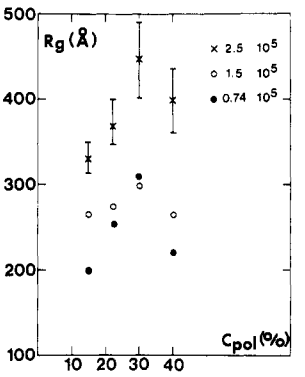

Figure 6. Variation of the chain radius of gyration as a function of the overall polymer concentration in iPS/*cis*-decalin gels. Labeled molecular weights as indicated.

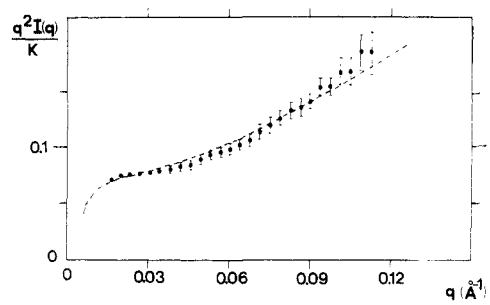

Figure 7. Kratky plot $q^2I(q)$ versus q for a 15% iPS/*cis*-decalin gel; $M_{w_{iPSD}} = 2.5 \times 10^5$, $C_{iPSD} = 0.01$ g/cm^3. Dashed line is calculated from the Yoshisaki and Yamakawa expression[21] by using $b = 80$ Å.

the degree of regular folding decreases with decreasing chain mobility, which results in a significant decrease of R_g.[20]

It is to be further noted that the maximum of R_g occurs at the same polymer concentration as C_γ, which corresponds to the polymer–compound stoichiometry. It accordingly seems that the stable form for the chain in the gel state at the stoichiometric composition is at a maximum extension. This statement is confirmed from the analysis of the intensity scattered in the intermediate domain.

For $C_{pol} = 15\%$, the scattered intensity can be satisfactorily fitted with a wormlike chain (Yamakawa and Yoshizaki calculation,[21] see Appendix) possessing a statistical segment of length 80 Å (Figure 7). This confirms previous conclusions drawn from the asymptotes only.[6] The same holds for $C_{pol} = 22.5\%$. Interestingly enough, if the linear mass μ_L is determined from the q^{-1} behavior after absolute calibration, one finds $\mu_L \simeq 52 \pm 2$ g/mol × Å. A 12_1 helix would give $\mu_L(12_1) = 44.1$ g/mol × Å (12 monomers for a pitch of 30.6 Å), while a 3_1 helical form would yield $\mu_L = 50.8$ g/mol × Å (three monomers for a pitch of 6.65 Å), a value much closer to the experimental one. Although taken alone this argument would not be decisive, it becomes more significant when considered with all the above results.

For $C_{pol} = 30\%$, the results are molecular weight dependent and are rather accounted for by using the calculation developed by Muroga[22] (see Appendix) on a model chain (contour length L) made up with long rods interrupted by smaller ones (see Appendix, relation 8A). There are three parameters: the length of the long rods (A), the fraction of these rods in the chain (f), and the length of the smaller rods (a). The method of trial and error has been employed here, that is, finding a combination of the above parameters that give a value of R_g as close as possible to the experimental one and fit the intensity in the asymptotic range. For $M_{w_{iPSD}} = 7.4 \times 10^4$ ($L \approx 1500$ Å), the best fit can be obtained by using $A = 400$ Å, $f = 80\%$, and $a = 40$ Å (Figure 8a). The value of R_g calculated from relation 12A in the Appendix is then $R_g = 278$ Å, a value in good agreement with the experimental one. For $M_w = 1.5 \times 10^5$ ($L \approx 3000$ Å), one ends up with $A = 450$ Å, $f = 45\%$, and $a = 40$ Å (Figure 8b), giving $R_g = 328$ Å, while for $M_w = 2.5 \times 10^5$ ($L \approx 5000$ Å), $A = 450$ Å, $f = 40\%$, and $a = 40$ Å (Figure 8c), leading to $R_g = 424$ Å. It must be stressed that other sets of values might certainly fit the data. However, there must always be large rods ($A > 300$ Å). Further, as already stressed above, the chain is virtually all extended for $M_w = 7.4 \times 10^4$. The pattern that would be obtained with a Hermans–Hermans model[23] with a statistical element of 200 Å determined from the values of R_g are also given as a comparison.

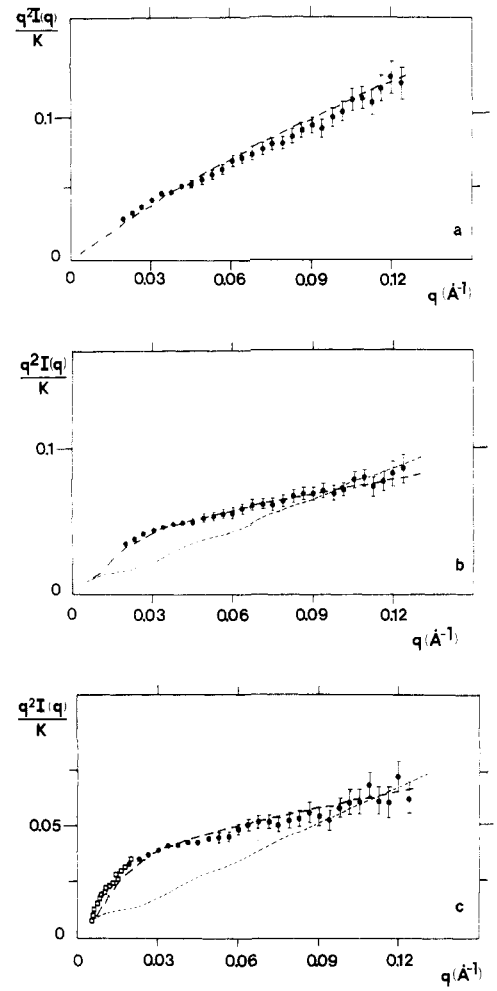

Figure 8. Kratky plot of $q_2I(q)$ versus q for iPS/*cis*-decalin gels (iPSK) prepared at 0 °C, $C_{pol} = 30\%$. (a) $M_{w_{iPSD}} = 7.4 \times 10^4$, $C_D = 0.01$ g/cm^3; dashed line correspond to relation 8A calculated with $A = 400$ Å, $a = 40$ Å, and $f = 0.8$. (b) $M_{w_{iPSD}} = 1.5 \times 10^5$, $C_D = 0.01$ g/cm^3; dashed line calculated with (8A) with $A = 450$ Å, $a = 40$ Å, and $f = 0.45$. Dotted line corresponds to the Hermans–Hermans model for $b = 200$ Å. (c) $M_{w_{iPSD}} = 2.5 \times 10^5$, $C_D = 0.01$ g/cm^3; dashed line calculated with (8A) with $A = 450$ Å, $a = 40$ Å, and $f = 0.4$. Dotted line corresponds to the Hermans–Hermans model for $b = 200$ Å. Open squares correspond to D11 data and full circles to D17 data.

The results on 30% gels in the Guinier range and in the asymptotic range are consistently accounted for with the model of Muroga. They lead one to conclude that the higher the labeled molecular weight, the larger the amount of "disorder". While it seems relatively easy for a short chain to become extended, this process seems more and more difficult for long chains. Here it is worth mentioning that molecular weight effects have already been observed when measuring mechanical properties such as the compression modulus.[24] These effects might thus arise from the variations in chain trajectories.

Experiments carried out for samples prepared at 14 °C instead of 0 °C have revealed little difference in the scattering pattern (see Figure 9). At this preparation temperature no liquid–liquid phase separation (LLPS) interferes with the gelation process. This indicates that the LLPS mechanism is not primarily responsible for the particular chain trajectory in iPS gels but that gelation is a phenomenon of its own.

For the sake of completeness it ought to be mentioned that we have so far neglected the corrective term exp-

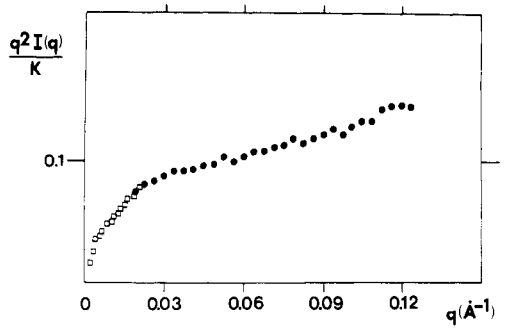

Figure 9. Kratky plot of $q^2I(q)$ versus q for a iPS/*cis*-decalin gel (iPSK) prepared at 14 °C, C_{pol} = 30%, M_{wiPSD} = 2.5 × 10^5, C_D = 0.018 g/cm^3. Open squares correspond to data from D11 and full circles to data from D17.

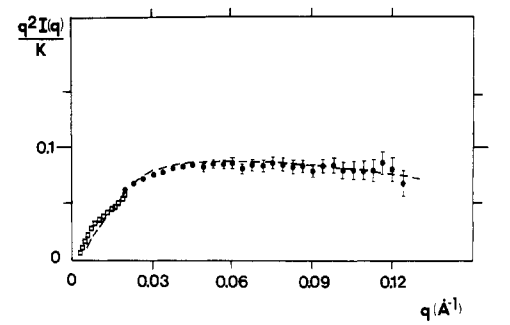

Figure 10. Kratky plot of $q^2I(q)$ versus q for a iPS/*cis*-decalin gel (iPSK) C_{pol} = 40%, M_{wiPSD} = 1.5 × 10^5, C_D = 0.01 g/cm^3; the dashed line stands for relation 8A calculated with A = 700 Å, a = 20 Å, and f = 28%. Open squares stand for D11 data, while full circle represent D17 data.

$(-q^2R^2_c/2)$, arising from the chain cross-section effect[25] (see Appendix). If the chain adopts a near-3_1 helical structure, then its outer radius R is $R \approx 3.5$ Å. The transverse radius of gyration of R_c of a cylinder full of matter with the same radius would be $R_c \approx 2.5$ Å. Here, the transverse radius of gyration R_c can only be lower. As a result, the corrective term can be ignored within the investigated range of scattering vectors.

For C_{pol} = 40%, the q^{-1} regime has totally vanished (Figure 10). A behavior close to $I(q) \approx q^{-2}$ is seen instead. Accounting for this behavior with a radius of gyration as large as that measured for C_{pol} = 15% requires the introduction of a cross-section effect as detailed in the Appendix. The best fit is then obtained with A = 700 Å, f = 28%, a = 20 Å, and R_c = 6 Å. One immediately realizes that a = 20 Å corresponds to the length of the statistical segment in the amorphous state. This is consistent with the fact that above 30% the stoichiometry is less and less fulfilled, which implies the probable appearance of "amorphous" material. The cross-section effect is not straightforwardly explained. It may arise from the fact that the long rods are not as straight as with C_{pol} < 30%, an effect that may be designated as superzigzag, entailing an increase of the filament cross section. Alternatively, folding may occur (hairpin conformations[26]), which is equivalent to an increase of chain cross section. More complex models containing rods of different lengths might also be more appropriate here. At any rate the important conclusion is that this result is consistent with the phase diagram:[7] increasing the concentration beyond C_γ entails the progressive disappearance of the conformations observed when the stoichiometry is fulfilled.

It must be stressed that a similar result (absence of a q^{-1} regime) has already been observed when a mixture of isomeric decalin (cis + trans) is used instead.[6] This

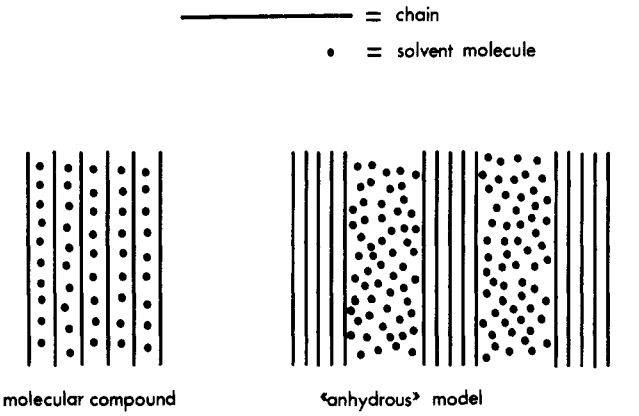

Figure 11. Schematic representation of the structure of the molecular compound (ladderlike model) and the "anhydrous" model.

was also interpreted with a superzigzag arising from the difference of interactions between *cis*-decalin molecules or *trans*-decalin molecules toward the polymer.

2. All the Chains Are Labeled (Deuterated). So far the results are rather consistent with the ladderlike model. Here we further test this model against models in which chains are more or less ordered but without solvent molecules. In Figure 11 are schematized two extreme models: the ladderlike model[4] for which the solvent is inserted between the polymer chains and the "anhydrous" model for which domains of pure polymer alternate with domains of pure solvent.

The latter model can be easily tested with an experiment on an all labeled samples. As a matter of fact one is then dealing with the two-density system that has been studied theoretically by Debye and Bueche.[27] The scattered intensity is simply

$$I(q) = K8\Pi d^2C(1 - C)N_A\zeta^3(1 + q^2\zeta^2)^{-2} \quad (14)$$

where ζ is the range of density fluctuation of the polymer density, C the proportion of polymer, and K the same constant as defined in (2). In the Kratky representation $(q^2I(q))$ a maximum should occur at

$$q\zeta = 1 \quad (15)$$

Conversely, in the case of the ladderlike model no q^{-4} variation should be found, but on the contrary, the q^{-1} behavior should reappear in spite of the all-labeled chain situation; the intensity is then given by[28]

$$I(q) \propto \frac{\pi}{qL}(1 + \int_0^R \Gamma(R)J_0(qR)\,dR) \quad (16)$$

where $\Gamma(R)$ is the distribution function normal to the rods. For $qR \gg 1$ relation 16 plotted by means of a Kratky plot tends to

$$q^2I(q) \propto \frac{\Pi q}{L} + A \quad (17)$$

in which A is a constant whose expression depends on $\Gamma(R)$. It is to be noted that here too a maximum should occur in the Kratky representation of relation 16 for qR < 1 whose location depends obviously upon $\Gamma(R)$.

The experimental intensity for the system considered reads

$$I(q) \propto X\bar{B}_{pol}{}^2S_{pol}{}^{coh}(q) + (1 - X)\bar{A}_{dec}{}^2S_{dec}{}^{coh}(q) + (1 - C_{pol})S_{dec}{}^{inc} \quad (18)$$

where X is the proportion of compound and the other terms have obvious meaning. Since we do not want to

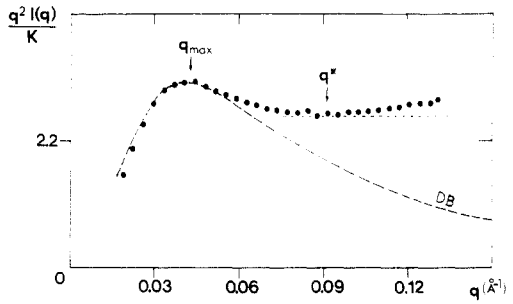

Figure 12. Kratky plot of $q_2I(q)$ versus q for an iPS/*cis*-decalin gel prepared at 0 °C, containing only deuterated chains ($M_{w_{iPSD}} = 2.5 \times 10^5$) in protonated *cis*-decalin. $C_{pol} = 32.8\%$. The dashed line (labeled DB) stands for the Debye–Bueche model for which $[\zeta]$ is determined from relation 15. The dotted line is a guide for the eyes to show the plateau value.

make any assumption as to the model for processing the raw data (value of X that amounts to either $X = C_{pol}$ with no compound or $X = 1$ with a pure compound), we have used deuterated polymer and hydrogenated decalin. As a matter of fact the coherent scattering length of decalin is virtually zero, which allows one to overcome the problem of substracting the proper coherent background for the solvent. As a result only the incoherent scattering, which is from pure decalin, has to be removed from the sample's intensity.

Results are reported in Figure 12 as a Kratky plot. As can be seen, q_{max} yields $\zeta \approx 24$ Å. By introducing this value in relation 14 the dashed line is obtained. The fit with the Debye–Bueche function is poor and totally incorrect in the high-q range. Further, the absolute intensity calculated from (14) should be about 10 times larger than the experimental one (in Figure 12 the Debye–Bueche function is therefore reduced by a factor of about 11.7 to fit the data in the low-q range).

It can be seen that there is a marked departure from the $1/q^2$ behavior, which may indicate that the rodlike behavior appears in the vicinity of $q^* \approx 0.09$ Å^{-1}. Studies are in progress to determine $\Gamma(R)$ from wide-angle experiments in order to fit $I(q)$.

One may wonder whether other models, intermediate between the two of Figure 11, could not also account for the data.

Instead of a sharp interface between the polymer domains and the solvent domains one can consider a model wherein the interface resembles a ladderlike model. The intensity scattered by this model should then be given by a modified Porod law at large angles:

$$I(q) \propto q^{-(6-d)} \tag{19}$$

in which d is the so-called fractal dimension of the interface with $d \leq 3$. If we consider the limiting case $d = 3$, then

$$I(q) \propto q^{-3} \tag{20}$$

Again this does not agree with the experimental results.

In a 30% polymer system, if there is a significant amount of "anhydrous" polymer domains then it is likely that "islands" of solvent will display high connectivity between one another. As a matter of fact, the concentration C^* at which spheres of radius R and mass M_s are isolated from one another ("swiss cheese" state) is given by the following relations, depending on whether one considers a cubic arrangement or a hexagonal one: cubic, $C^* = M_s/8R^3$; hexagonal $C^* = M_s/6R^3$.

Since $M_s = d_s 4\pi R^3/3$ where d_s is the density of the solvent in the present case, this eventually leads to the following relationships: cubic, $C^* \approx 0.52d_s$; hexagonal, $C^* \approx 0.7d_s$. In practice C^* will be located between these two limiting values.

If such were the case for the gel under consideration, then it should be described as a bicontinuous medium. According to Talmon and Prager,[29] although no simple exponent law can be found, the intensity first decreases faster than $1/q^4$ and then reaches this type of behavior.

To summarize, all the models examined here, which contain domains of pure polymer, cannot account for the experimental results.

Concluding Remarks

In this paper we again show that the 12_1 helical form is not characteristic of the iPS gels in the nascent state. Instead, we continue to suggest on the basis of simple considerations that the systems are made up of near-3_1 helices that are solvated (ladderlike model). The solvation assumption is in agreement with the phase diagrams[7] as well as with the swelling experiments.

Further, the chain conformation is totally different from what is observed in the semicrystalline state.[19,20] In particular for $C < C_\gamma$, the chains tend to possess long rodlike sections of length far larger than what is known for chain-folded crystals. Beyond C_γ the chains do not exhibit the scattering pattern seen at lower concentrations. This is in agreement with the phase diagram that shows the disappearance of the compound above C_γ.[7] In our opinion, only the helix solvation process can explain the absence of chain folding and correspondingly the existence of long rod portions (helix stabilization).

Here the dismissal of the solvation hypothesis by Perez et al.[5] on the basis of NMR experiments is worth discussing again. Put to the test with an all-labeled sample, the ladderlike model accounts for the results far better. One may, however, wonder why NMR on the one hand and several other techniques on the other hand (DSC, neutron scattering, swelling experiments) lead one to opposing models. Two reasons might be invoked:

(i) NMR deals with the "dynamic" structure, which is not necessarily equivalent to the "static" structure, the time-averaging not being the same. In elastic neutron scattering experiments, which allow one to probe shorter times, might be more relevant to study this problem.

(ii) NMR results were obtained on a high molecular weight sample ($M_w \approx 1.4 \times 10^6$).[5] We have shown here that at $C = 30\%$ the chain conformation is molecular weight dependent within less than a decade. In particular, the higher the molecular weight the larger the degree of "disorder" (incidentally this phenomenon is also known for semicrystalline polymers[20,30]). One may then wonder whether NMR results obtained on such a high molecular weight sample are representative of the gel state as deduced from studies on samples of lower molecular weight. Clearly, is the argument about the same thing? This point deserves to be further tested.

Finally, it seems worth mentioning that similar solvent effects between *cis*-decalin and *trans*-decalin have been observed for physical gels prepared from steroids.[31] Similar mechanisms might be involved here too.

Appendix

1. Form Factor for a Wormlike Chain. Theoretical calculations of the form factor $P(q)$ of a wormlike chain were first derived by Kratky et al.[32] and more recently by Des Cloizeaux[33] and Yamakawa and Yoshisaki.[21] In the limit of very long chains, two asymptotic regimes are expected in the intermediate range:

$$\text{regime 1} \qquad (L/a)P_1(q) \simeq 6/q^2a^2 \tag{1A}$$

$$\text{regime 2} \qquad (L/a)P_2(q) \simeq \pi/qa + 2/3(qa)^2 \quad (2A)$$

where a represents the persistence length and L the chain contour length. If q^* is defined as being the intersect in the Kratky representation between the asymptotes of $q^2P_1(q)$ and $q^2P_2(q)$, then q is straightforwardly

$$q^* = 16/3\pi a \simeq 1.7/a \quad (3A)$$

Similarly, one can define q_0, which is the value of the abcissa at which $q^2I(q) = 0$:

$$q_0 = -2/(3\pi a) \quad (4A)$$

If the statistical segment b is considered instead, which is by definition of the persistence length $b = 2a$, one ends up with

$$\text{regime 1} \qquad (L/b)P_1(q) \simeq 12/q^2b^2 \quad (5A)$$

$$\text{regime 2} \qquad (L/b)P_2(q) \simeq \pi/qb + 4/3(qb)^2 \quad (6A)$$

This gives for q^* and q_0:

$$q^* = 32/3\pi b \quad \text{and} \quad q_0 = -4/(3\pi b) \quad (7A)$$

It is to be noted that Yamakawa and Yoshizaki have derived an analytical expression allowing numerical calculation to be performed up to $qb = 10$.[21]

2. Form Factor of a Copolymer-Like Model. Here we consider the model developed by Muroga.[22] In this model long rods are joined together by a flexible portion made up of smaller rods, which is reminiscent of a block copolymer except that in this model the scatterers are of identical chemical nature. When the amount of flexible portion is taken as zero, this model reduces to the well-known Hermans and Hermans model of freely jointed rods.[23]

For a chain of contour length L, containing N rods of length A alternating with subunits containing n rods of length a, these subunits being assimilated to random coils characterized by an end-to-end distance na^2, Muroga derived the following analytical expression of $P(\theta)$:

$$L^2P(\theta) = NA^2\left\{2\Lambda(\beta) - \frac{4}{\beta^2}\sin^2\frac{\beta^2}{2}\right\} + 2NA^2\Lambda^2(\beta) \times \left\{\frac{\exp(-\omega)}{1-\nu\exp(-\omega)}\right\} - 2A^2\Lambda^2(\beta)\left\{\frac{\exp(-\omega)}{1-\nu\exp(-\omega)}\right\} \times \left\{\frac{1-(\nu\exp(-\omega))^N}{1-\nu\exp(-\omega)}\right\} + n^2N^2a^2\left\{\frac{2}{N\omega} - 2\left(\frac{1-\exp(-\omega)}{N\omega}\right)^2 \times \left(\frac{\nu}{1-\nu\exp(-\omega)}\right)\left(\frac{1-(\nu\exp(-\omega))^N}{1-\exp(-\omega)}\right) - 2\frac{(1-\exp(-\omega))(1-\nu)}{N\omega^2(1-\nu\exp(-\omega))}\right\} + \frac{2naA\Lambda(\beta)(1-\exp(-\omega))}{\omega(1-\nu\exp(-\omega))} \times \left\{2N - \frac{(1+\nu\exp(-\omega))(1-(\nu\exp(-\omega))^N)}{1-\nu\exp(-\omega)}\right\} \quad (8A)$$

where ω, β, and ν are defined as $\omega = qna^2/6$, $\beta = qA$, and $\nu = \sin\beta/\beta$ and $\Lambda(\beta)$ as

$$\Lambda(\beta) = (1/\beta)\int_0^\beta \sin t/t\, dt = (1/\beta)\,\mathrm{Si}\,(\beta)$$

The fraction f of rods with length A is given by $f = NA/L$.

As stated above, by taking $a = 0$, one retrieves the Hermans and Hermans model,[23] for which $P(\theta)$ is

$$L^2P(\theta) = NA^2\left\{2\Lambda(\beta) - \frac{4}{\beta^2}\sin^2\frac{\beta^2}{2}\right\} + 2NA^2\Lambda^2(\beta) \times \left\{\frac{\exp(-\omega)}{1-\nu\exp(-\omega)}\right\} - 2A^2\Lambda^2(\beta)\left\{\frac{1-\nu^N}{(1-\nu)^2}\right\} \quad (9A)$$

Note that the asymptotic value of (9A) is for $qR > 1$ and $qA > 1$[34]

$$\frac{L}{b}P(q) = \frac{\pi}{qb} + \left(\frac{\pi^2}{2} - 4\right)\frac{1}{q^2b^2} \quad (10A)$$

This shows that the intercept of the q^{-1} behavior with the ordinate axis is slightly above what one would obtain with a wormlike chain.

Muroga gives, however, only an approached expression of the chain radius of gyration R_g by developing the form factor for $q \to 0$.

Given a slight modification, the model developed for Muroga is similar to the Garland model, which is a crystalline model for chains containing amorphous sequences that alternate with crystalline ones made up of several parallel rods.[35] Here one has to consider only one rod per crystalline sequence. The radius of gyration R_g for this model is

$$R_g^2 = (1-f)R_A^2 + (Mf/6\mu_R)l_c^2 \quad (11A)$$

where R_A^2 is the radius of gyration for a chain in the totally disordered state (which is also its unperturbed state with a statistical segment of length a), μ_R the molecular weight of a rod of length A ("ordered" region), and f the proportion of such rods. By introduction of $\lambda = A/a$, the chain molecular weight M, and the linear mass μ_L, the latter being further assumed independent of the statistical length, R_g^2 is

$$R_g^2 = [(1-f) + f\lambda]Ma/6\mu_L \quad (12A)$$

or by introduction of the contour length L

$$R_g^2 = [(1-f) + f\lambda]aL/6 \quad (13A)$$

3. Effect of Chain Cross Section. So far an infinitely thin thread has been considered. In reality, polymer chains possess a finite cross section, which must be taken into account. If the transverse chain shape possesses a cylindrical symmetry, then the corrected expression for $P(q)$ is[36]

$$P(q) = P_0(q)\frac{4J_1^2(qr)}{(qr)^2} \quad (14A)$$

where $P_0(q)$ is the form factor when the cross-section diameter $2r = 0$. The Bessel function can be developed for $qr < 1$, which eventually gives

$$P(q) = P_0(q)\exp(-q^2R_c^2/2) \quad (15A)$$

where R_c^2 is the radius of gyration of the cross-sectional area.

Registry No. iPS, 25086-18-4; *cis*-decalin, 493-01-6; neutron, 12586-31-1; 1-chlorodecane, 1002-69-3; hexahydroindanH, 496-10-6; *trans*-decalinH, 493-02-7.

References and Notes

(1) Girolamo, M.; Keller, A.; Miyasaka, K.; Overbergh, N. *J. Polym. Sci., Polym. Phys. Ed.* **1976**, *14*, 39.

(2) Atkins, E. D. T.; Isaac, D. M.; Keller, A. *J. Polym. Sci., Polym. Phys. Ed.* **1980**, *18*, 71. Atkins, E. D. T.; Keller, A.; Shapiro, J. S.; Lemstra, P. J. *Polymer* **1981**, *22*, 1161.

(3) Sundararajan, P. R.; Tyrer, N. J.; Bluhm, T. L. *Macromolecules* **1982**, *15*, 286.
(4) Guenet, J. M. *Macromolecules* **1986**, *19*, 1961.
(5) Perez, E.; Vanderhart, D. L.; McKenna, G. B. *Macromolecules* **1988**, *21*, 2418.
(6) Guenet, J. M. *Macromolecules* **1987**, *20*, 2874.
(7) Guenet, J. M.; McKenna, G. B. *Macromolecules* **1988**, *21*, 1752.
(8) Natta, G. *J. Polym. Sci.* **1955**, *16*, 143.
(9) Guenet, J. M.; Gallot, Z.; Picot, C.; Benoit, H. *J. Appl. Polym. Sci.* **1977**, *21*, 2181.
(10) Atkins, E. D. T.; et al. *Colloid Polym. Sci.* **1984**, *262*, 22.
(11) Bellissent, R.; Chenevas-Paule, A.; Roth, M. *J. Non-Cryst. Solids* **1983**, *59-60*, 229.
(12) See, for instance: Guinier, A. In *Théorie et Technique de la Radiocristallographie*; Dunod: Paris, 1955.
(13) Natta, G.; Corradini, P.; Bassi, I. W. *Suppl. Nuovo Cimento* **1960**, *15*, 68.
(14) Watanabe, J.; Sasanuma, Y.; Endo, A.; Uematsu, I. *Rep. Prog. Polym. Phys. Jpn.* **1980**, *23*, 667.
(15) He, X.; Herz, J.; Guenet, J. M. *Macromolecules* **1987**, *20*, 2003.
(16) Zimm, B. H. *J. Chem. Phys.* **1948**, *16*, 1093.
(17) Daoud, M.; et al. *Macromolecules* **1975**, *8*, 804.
(18) Sadler, D. M.; Keller, A. *Macromolecules* **1977**, *10*, 1128.
(19) Guenet, J. M. *Macromolecules* **1980**, *13*, 380.
(20) Guenet, J. M. *Polymer* **1981**, *22*, 313.
(21) Yoshisaki, T.; Yamakawa, H. *Macromolecules* **1980**, *13*, 1518.
(22) Muroga, Y. *Macromolecules* **1988**, *21*, 2751.
(23) Hermans, J.; Hermans, J. J. *J. Phys. Chem.* **1958**, *62*, 1543.
(24) McKenna, G. B.; Guenet, J. M. *Polym. Commun.* **1988**, *29*, 58.
(25) Rawiso, M.; Duplessix, R.; Picot, C. *Macromolecules* **1987**, *20*, 630.
(26) de Gennes, P.-G. In *Polymer Liquid Crystals*; Academic Press: New York, 1982.
(27) Debye, P.; Bueche, A. M. *J. Appl. Phys.* **1949**, *20*, 518.
(28) Sadler, D. M.; Harris, R. *J. Polym. Sci., Polym. Phys. Ed.* **1982**, *20*, 561.
(29) Talmon, Y.; Prager, S. *J. Chem. Phys.* **1978**, *69*, 2984.
(30) See, for instance: Hoffman, J. D.; Davis, G. T.; Lauritzen, J. I., Jr. In *Treatise on Solid State Chemistry*; Hanney, N. B., Ed.; Plenum: New York; Chapter 7.
(31) Terech, P., private communication, to be submitted.
(32) Heine, S.; Kratky, O.; Porod, G.; Schmitz, J. P. *Makromol. Chem.* **1961**, *44*, 682.
(33) Des Cloizeaux, J. *Macromolecules* **1973**, *6*, 403.
(34) Luzzati, V.; Benoit, H. *Acta Crystallogr.* **1961**, *14*, 297.
(35) Guenet, J. M. *Polymer* **1980**, *21*, 1385.
(36) Porod, G. *Kolloid Z.* **1951**, *124*, 83; **1952**, *125*, 51.

Forces between Surfaces with Adsorbed Polymers. 3. Θ Solvent. Calculations and Comparison with Experiment

Kevin Ingersent,[†] Jacob Klein,*[,‡] and Philip Pincus[§]

Magdalene College, Cambridge, England, Polymer Department, Weizmann Institute of Science, Rehovot 76100, Israel, and Corporate Laboratories, Exxon Research and Engineering Corporation, Clinton Township, Annandale, New Jersey 08801.
Received December 20, 1988; Revised Manuscript Received June 26, 1989

ABSTRACT: The adsorption of polymers onto a surface from a Θ solvent is treated in terms of a mean-field model based on a Cahn–de Gennes approach. In particular, we calculate the forces between two such polymer bearing surfaces and compare our results in some detail with available experimental data on force profiles between mica surfaces bearing adsorbed polymer near the Θ temperature. All parameters in our model may be estimated from experiment. The predicted force profiles are in very good qualitative agreement with the experimental data, though the absolute spatial and energy scales are smaller for the calculated profiles by factors of ca. 4 and 2.5 relative to experiment. The causes of this discrepancy and possible improvements to the model are considered.

I. Introduction

The technological importance of colloid stabilization and destabilization (or flocculation) by polymers has resulted in extensive experimental and theoretical studies of polymer adsorption and the resulting force between two coated surfaces; the situation to about 1982 is summarized in comprehensive reviews.[1,2] Generally, the adsorption free energy of a high molecular weight polymer attracted to an interface greatly exceeds thermal energies, leading to a quasi-irreversible attachment; i.e., after a long incubation of a surface in contact with a polymer solution, the solution may be replaced by pure solvent with negligible reduction of the surface excess (in the case of polymers that are very marginally adsorbed, some desorption may occur on washing). When two such surfaces are brought together, the mutual interaction arises from a balance between (attractive) bridging and the increased osmotic polymer–polymer coupling resulting from the augmented concentration between the plates. Thus, it is not surprising that the disjoining pressure is very sensitive to the structure of the segment distribution for adsorbed polymers.

For a single surface, the interfacial structure of adsorbed polymers has been actively investigated in recent years. Theoretically, Scheutjens and Fleer[3] have applied the transfer matrix formalism,[4] in conjunction with a Flory–Huggins free-energy functional for the polymer solution. Bulk polymer solution properties in good solvents often differ appreciably from mean-field results, in close analogy to critical phenomena;[5] in order to ensure compatibility with bulk properties, de Gennes[6] generalized the Cahn approach[7] for interfacial energies to obey correct scaling relations for polymer solutions. The boundary condition at the interface used in this scaling theory for

[†] Magdalene College. Present address: Department of Physics, University of Pennsylvania, Philadelphia, PA 19104.
[‡] Polymer Department, Weizmann Institute of Science, Rehovot 76100, Israel. Incumbent of Herman Mark Chair in Polymer Physics.
[§] Exxon Research and Engineering Corporation. Present address: Department of Materials Science, University of California at Santa Barbara, Santa Barbara, CA 93106.

0024-9297/90/2223-0548$02.50/0